THE JOURNAL OF BIOLOGICAL CHEMISTRY
Vol. 280, No. 11, Issue of March 18, pp. 10253–10263, 2005

Printed in U.S.A.

Platelet-derived Growth Factor Stimulates Src-dependent mRNA Stabilization of Specific Early Genes in Fibroblasts*

Received for publication, December 8, 2004, and in revised form, December 21, 2004
Published, JBC Papers in Press, January 5, 2005, DOI 10.1074/jbc.M413806200

Paul A. Bromann‡, Hasan Korkaya‡, Craig P. Webb§, Jeremy Miller§, Tammy L. Calvin‡, and Sara A. Courtneidge‡¶

From the ‡Laboratory of Signal Regulation and Cancer, and §Laboratory of Tumor Metastasis and Angiogenesis, Van Andel Research Institute, Grand Rapids, Michigan 49503

The Src family of protein-tyrosine kinases (SFKs) participates in a variety of signal transduction pathways, including promotion of cell growth, prevention of apoptosis, and regulation of cell interactions and motility. In particular, SFKs are required for the mitogenic response to platelet-derived growth factor (PDGF). However, it is not clear whether there is a discrete SFK-specific pathway leading to enhanced gene expression or whether SFKs act to generally enhance PDGF-stimulated gene expression. To examine this, we treated quiescent NIH3T3 cells with PDGF in the presence or absence of small molecule inhibitors of SFKs, phosphatidylinositol 3-kinase (PI3K), and MEK1/2. Global patterns of gene expression were analyzed by using Affymetrix GeneChip arrays, and data were validated by using reverse transcription-PCR and ribonuclease protection assay. We identified a discrete set of immediate early genes induced by PDGF and inhibited in the presence of the SFK-selective inhibitor SU6656. A subset of these SFK-dependent genes was induced by PDGF even in the presence of the MEK1/2 inhibitor U0126 or the PI3K inhibitor LY294002. By using ribonuclease protection assays and nuclear run-off assays, we further determined that PDGF did not stimulate the rate of transcription of these SFK-dependent immediate early genes but rather promoted mRNA stabilization. Our data suggest that PDGF regulates gene expression through an SFK-specific pathway that is distinct from the Ras-MAPK and PI3K pathways, and that SFKs signal gene expression by enhancing mRNA stability.

The protein-tyrosine kinase Src was first described more than 20 years ago. It is the prototype for a group of nonreceptor tyrosine kinases, the Src family. Some members of this family are restricted in their expression to hematopoietic cells, whereas others (Src, Fyn, and Yes) are more ubiquitously expressed. SFKs[1] help to transduce signals from a variety of cell surface receptors during proliferative and immune responses. They are also frequently activated as cells enter mitosis, rearrange their cytoskeleton, or become motile (1–3). Thus, they are involved in a diverse array of physiological processes.

Much of the understanding of SFK function comes from analyses of fibroblasts in culture. These studies established that SFKs participate in the mitogenic response elicited by several peptide growth factors, including epidermal growth factor (EGF) and PDGF (4). SFKs become activated when fibroblasts are stimulated with PDGF, whose receptor is itself a tyrosine kinase (5), and associate with the PDGF receptor (PDGF-R) (6, 7). SFKs are required for PDGF to stimulate mitogenesis in NIH3T3 cells (8, 9). Our laboratory has recently focused on the growth factor-stimulated production of Myc, a transcription factor required for efficient cell cycle transit. Previous work demonstrated that the block to PDGF-stimulated DNA synthesis caused by dominant negative SFKs could be overcome by expression of Myc (10). Another transcription factor, Fos, was unable to rescue this block. Furthermore, Myc could not overcome the block caused by dominant negative Ras. Together, these data suggested that PDGF stimulation results in the initiation of a discrete SFK signal transduction pathway, distinct from the classical Ras-MAPK pathway, which culminates in Myc production. The subsequent characterization and use of SU6656, an SFK inhibitor, confirmed that *myc* mRNA was in large part under SFK control (9).

These studies have suggested that different PDGF effectors might each control a discrete subset of the response of the cell to PDGF. However, one study reported that activation of PDGF-R led to enhanced expression of a set of immediate early genes, and that PDGF-R mutants lacking binding sites for individual signaling effectors (including Ras-GAP or PI3K) failed to block expression of any of these genes (11). These data suggested a lack of specificity in PDGF-R signaling. We decided to address this issue by using a different approach: analyzing global patterns of gene expression in quiescent fibroblasts stimulated with PDGF in the presence or absence of various small molecule inhibitors. These studies are reported here.

EXPERIMENTAL PROCEDURES

Cell Line and Reagents—NIH3T3 fibroblast cells were maintained in Dulbecco's modified Eagle's medium with 2 mM L-glutamine, 1.5 mg/ml glucose, 100 units/ml penicillin, 100 μg/ml streptomycin, and 10% heat-inactivated fetal bovine serum. Recombinant human PDGF-BB was purchased from Upstate Biotechnology, Inc. (Lake Placid, NY). SU6656 was obtained from SUGEN, Inc. (South San Francisco, CA), and U0126, PD98059, and LY294002 were purchased from EMD Biosciences, Inc. (La Jolla, CA). Radionuclides were purchased from Amersham Biosciences (Piscataway, NJ), and all other molecular biology reagents were purchased from Invitrogen (Carlsbad, CA). Murine Genome

* This work was supported by the Van Andel Research Institute. The costs of publication of this article were defrayed in part by the payment of page charges. This article must therefore be hereby marked "*advertisement*" in accordance with 18 U.S.C. Section 1734 solely to indicate this fact.

¶ To whom correspondence should be addressed: Laboratory of Signal Regulation and Cancer, Van Andel Research Institute, 333 Bostwick NE, Grand Rapids, MI 49503. Tel.: 616-234-5704; Fax: 616-234-5705; E-mail: sara.courtneidge@vai.org.

[1] The abbreviations used are: SFKs, Src family kinases; PI3K, phosphatidylinositol 3-kinase; PDGF, platelet-derived growth factor; PDGF-R, PDGF receptor; MAPK, mitogen-activated protein kinase; MEK, MAPK kinase; EGF, epidermal growth factor; RPA, ribonuclease protection assay; RT, reverse transcription; UTR, untranslated region; CRD, CR instability determinant; AUREs, AU-rich elements; probe IDs, probe identification.

U74v2 set and Mouse Expression set 430 GeneChip arrays were purchased from Affymetrix (Santa Clara, CA).

PDGF Stimulation and RNA Isolation—NIH3T3 cells were seeded at 7×10^5 cells/10-cm plate and grown at 37 °C in 5% CO_2, 95% O_2 for 24 h. Cells were then quiesced for 40 h in starvation medium (Dulbecco's modified Eagle's medium with 2 mM L-glutamine, 1.5 mg/ml glucose, 100 units/ml penicillin, 100 μg/ml streptomycin, 0.5% fetal bovine serum, and 1× insulin/transferrin/selenium (Invitrogen)). After 40 h, quiescent cells were placed in fresh starvation medium for an additional 30 min. Cells were then incubated with SU6656 (2 μM), U0126 (10 μM), LY294002 (7.5 μM), PD98059 (50 μM), or Me_2SO vehicle for 1 h. Then, in the presence of inhibitors or vehicle, cells were stimulated for 1 h with 25 ng/ml PDGF-BB. Total RNA was isolated using either Trizol reagent (Invitrogen) or RNeasy mini kits (Qiagen, Valencia, CA) according to the manufacturers' instructions. The quality of the total RNA was analyzed by measuring the A_{260}/A_{280} ratio as well as the intensity of 18 S and 28 S rRNA on a 1% agarose gel.

Affymetrix GeneChip Analysis—The Affymetrix protocol followed was essentially as described previously (12). Briefly, 100 pmol of a T7-$(dT)_{24}$ primer was added to 10 μg of total RNA. The primer and RNA were denatured at 70 °C for 10 min and placed on ice, and cDNA was then synthesized by using SuperScript II RT (Invitrogen) according to the manufacturer's instructions. Reactions were terminated by addition of EDTA to a final concentration of 30 mM, and samples were placed on ice. An equal volume of phenol/chloroform/isoamyl alcohol (25:24:1) was added to each cDNA sample, transferred to Phase Lock gels (Eppendorf Scientific, Westbury, NY), and centrifuged at 16,000 × *g* for 2 min. The aqueous upper layer was precipitated with 2.5 M ammonium acetate and 2.5× final volume 100% ethanol. Samples were centrifuged, and resulting pellets were washed extensively with 80% ethanol and resuspended in 12 μl of diethyl pyrocarbonate-treated water.

The *in vitro* transcription labeling reactions were done using the ENZO BioArray kit (Affymetrix) to synthesize amplified biotin-labeled cRNA targets. The labeled cRNA was cleaned using RNeasy mini kits, and 15 μg was hybridized to Murine Genome U74Av2 or Mouse Expression 430 GeneChip arrays at the Genomics Technology Support Facility at Michigan State University (East Lansing, MI) on a GeneChip Scanner 3000 (Affymetrix). Probe intensity values were extracted from the array image using GCOS software (Affymetrix). All of the Affymetrix GeneChip array expression data have been deposited in the NCBI gene expression and hybridization array data repository (accession number GSE2196).

Data Analysis—Affymetrix gene expression data were normalized to an average intensity of 500 across each array, and the normalized CHP files were entered into xenobase, a relational database with associated analysis software (www.vai.org/vari/xenobase/default.asp). Data from corresponding quiescent NIH3T3 samples were selected as reference to allow calculation of treated/quiescent gene expression ratios. Gene expression ratios were $\log_2$-transformed prior to analysis so that relative increases and decreases in gene expression were represented on a linear scale. For genes called absent in test and reference samples, no fold change in gene expression was calculated. For hierarchical clustering of gene expression profiles, $\log_2$-transformed gene expression ratios were loaded into and viewed with xenobase, and average linkage clustering was carried out using correlation coefficients as described (13).

Semi-quantitative RT-PCR—Unique oligonucleotide primer pairs were designed using Unigene sequence data from the NCBI database, and oligonucleotides were obtained from IDT DNA Technologies (Coralville, IA). Five μg of RNeasy mini kit-purified total RNA was reverse-transcribed with SuperScript II RT using oligo(dT) primers (Invitrogen) according to the manufacturer's instructions. Two μl of cDNA per reaction were amplified by PCR using gene-specific primers as follows: 94 °C (2 min); 19–24 cycles of 94 °C (1 min), 55 °C (30 s), and 72 °C (1 min). PCRs were performed in duplicate or triplicate, and products were visualized by using 2% agarose gel electrophoresis. Amplification of β-actin was used as an internal control.

Ribonuclease Protection Assay (RPA)—Quiescent NIH3T3 cells were stimulated with 25 ng/ml PDGF in the presence of small molecule inhibitors. Total RNA was isolated using the RNeasy mini kit (Qiagen). For each reaction, 25 μg of total RNA was mixed with ^{32}P-labeled riboprobes, which were transcribed from restriction-digested plasmid DNA using the MAXIScript T7 kit from Ambion, Inc. (Austin, TX). RPAs were performed using the RPA III kit from Ambion according to the manufacturer's instructions. Protected fragments were resolved by PAGE using Criterion 5% TBE urea precast gels (Bio-Rad). After PAGE, gels were transferred to filter paper, vacuum-dried, and exposed to x-ray film for 1–6 h. Films were processed in a Kodak film developer and scanned into Adobe Photoshop 7.0 for digital imaging.

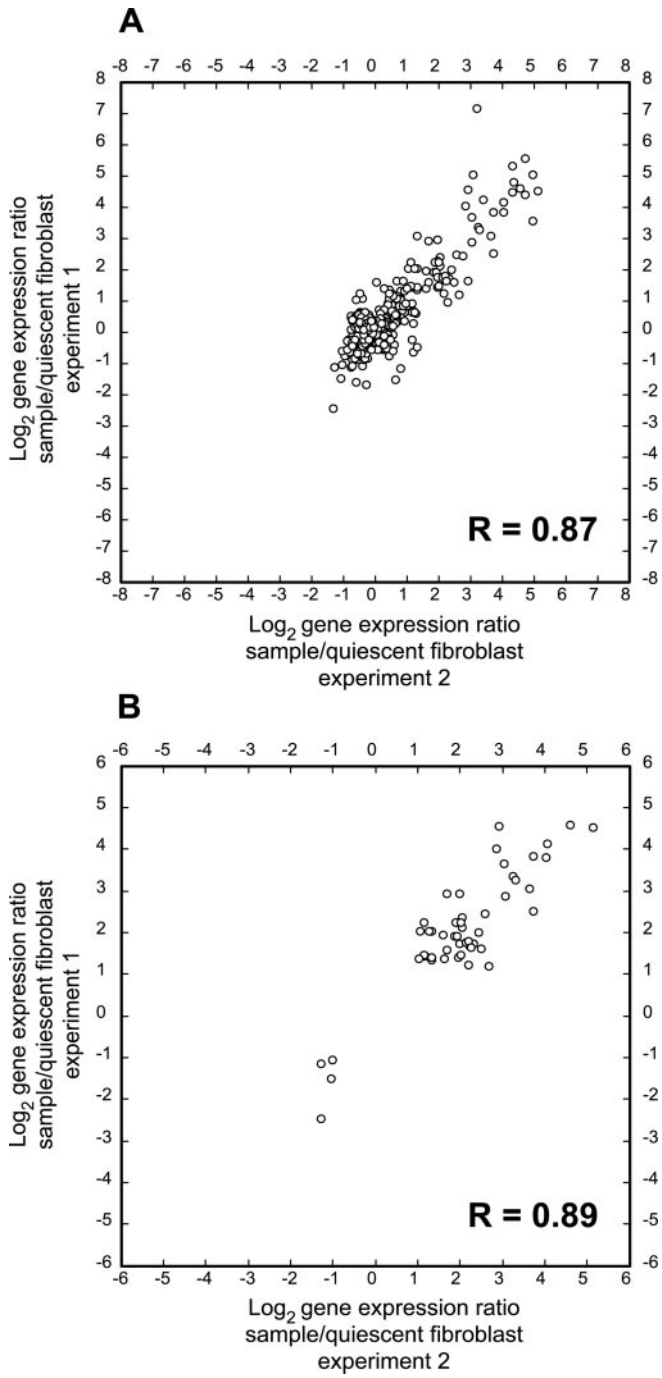

FIG. 1. **Reproducibility of Affymetrix GeneChip gene expression data.** Quiescent NIH3T3 cells were treated for 1 h with 25 ng/ml PDGF or vehicle in two separate identical experiments. Global patterns of gene expression were identified using Affymetrix Murine Genome U74Av2 GeneChip arrays, and gene expression ratios were $\log_2$-transformed prior to analysis so that relative increases and decreases in gene expression are represented on a linear scale. *A*, the $\log_2$-transformed gene expression ratios from experiment 1 (sample/quiescent fibroblast) were plotted against the $\log_2$-transformed gene expression ratios from experiment 2 with a correlation coefficient of 0.87. *B*, the same analysis was done for probe IDs that changed expression levels at least 2-fold in response to PDGF between experiment 1 and 2 with a correlation coefficient of 0.89.

Nuclear Run-off Assay—Quiescent NIH3T3 cells were stimulated with 25 ng/ml PDGF for 0–60 min. Cells were washed twice in phosphate-buffered saline, scraped into ice-cold phosphate-buffered saline, and centrifuged at 1000 rpm at 4 °C. The cell pellets were then resuspended in 500 μl of ice-cold RSB buffer (10 mM Tris, pH 7.5, 10 mM NaCl, 5 mM $MgCl_2$, 1 mM dithiothreitol, and 1% Nonidet P-40). After 5 min of incubation on ice, the cells were disrupted by Dounce homoge-

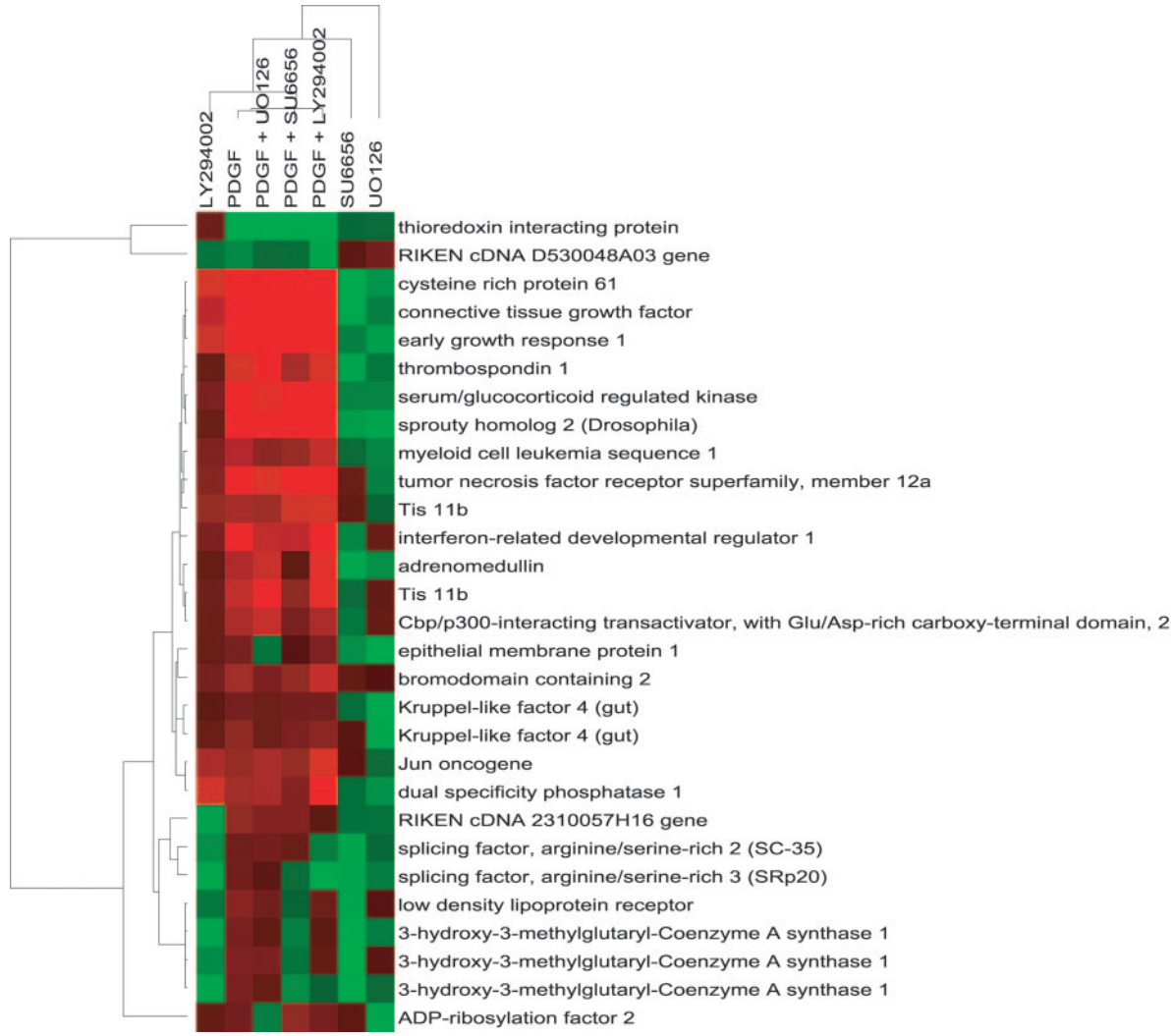

FIG. 2. **Unsupervised hierarchical clustering of Affymetrix GeneChip gene expression data.** Quiescent NIH3T3 cells were treated for 1 h with 25 ng/ml PDGF or vehicle in the presence of 2 μM SU6656, 10 μM U0126, 7.5 μM LY294002, or vehicle. Global patterns of gene expression were identified using Affymetrix Murine Genome U74Av2 GeneChip arrays, and gene expression ratios were $\log_2$-transformed prior to analysis so that relative increases and decreases in gene expression are represented on a linear scale. These data were subjected to unsupervised hierarchical clustering so that changes in gene expression across samples could be readily observed. *Red* and *green boxes* indicate relative high and low expression, respectively, for the given probe ID.

nization, and nuclei were isolated by centrifugation for 5 min at 2000 rpm at 4 °C. The nuclei were resuspended in 2 ml of ice-cold reaction buffer (20 mM Tris, pH 7.5, 10 mM $MgCl_2$, 140 mM KCl, 1 mM dithiothreitol, and 20% glycerol) and pelleted by centrifugation for 5 min at 2000 rpm at 4 °C. The nuclei were then resuspended in 200 μl of ice-cold reaction buffer containing 5 mM each of ATP, CTP, GTP, and 25 μCi of [α-^{32}P]UTP. Following 10 min of incubation at 37 °C, the nascent RNA was extracted using Trizol and hybridized to specific DNA probes blotted on Hybond-N membrane (Amersham Biosciences).

To prepare DNA probes, 400–600-bp DNA fragments from mouse *mcp-1*, *mcp-3*, *myc*, *adrenomedullin*, *fos*, and *β-actin* were amplified by PCR using gene-specific primer pairs. Ten μg of PCR product were denatured by incubating in 100 mM NaOH at 100 °C for 10 min. Denatured DNA samples and nonspecific probes were applied to nitrocellulose membrane using Bio-Dot apparatus (Bio-Rad). The membrane was then air-dried and UV cross-linked (1200 μJ) using a Stratalinker (Stratagene).

Immunoblotting—To detect ERK1/2 and phospho-ERK1/2, NIH3T3 cells were treated as described above and suspended in lysis buffer (20 mM Tris, pH 7.6, 150 mM NaCl, 1% Triton X-100, 10% glycerol, 10 mM NaF, 0.1 mM Na_3VO_4, 10 mM $Na_4P_2O_7$, 10 mM EDTA, and protease inhibitors). Protein bands were resolved by SDS-PAGE and transferred to Hybond-ECL nitrocellulose membranes (Amersham Biosciences). Membranes were blocked in TBST (50 mM Tris-HCl, pH 7.5, 150 mM NaCl, and 0.1% Tween 20) containing 5% milk and incubated overnight at 4 °C with anti-phospho-ERK1/2 mouse monoclonal antibody (E-4), stripped, and reprobed using anti-ERK1/2 rabbit polyclonal antibody (C-16, Santa Cruz Biotechnology, Santa Cruz, CA). Bound antibodies were detected using horseradish peroxidase-linked secondary antibodies (Sigma) and detected using SuperSignal West Pico chemiluminescent substrate (Pierce).

RESULTS

Patterns of Gene Expression in NIH3T3 Fibroblasts Are Experimentally Reproducible—To identify global patterns of PDGF-induced immediate early gene expression in NIH3T3 cells, quiescent cells were treated for 1 h with 25 ng/ml PDGF-BB or with vehicle. Two separate but identical experiments were performed, and the total RNA from each was hybridized to Affymetrix Murine Genome (MG) U74Av2 GeneChip arrays as described under "Experimental Procedures." Because only low passage (less than 10 passages) NIH3T3 cells were used in these studies, and because identical conditions were used in each experiment, a high degree of data reproducibility between experiments was expected.

To eliminate low intensity noise, we analyzed gene expression data from both experiments using the following filters: gene expression values were present in all samples, and sample intensity values were greater than 150 units and differed by more than 350 intensity units from quiescent NIH3T3 reference. For experiment 1, this filtering resulted in the identification of 538 sample probe IDs that differed from the reference.

TABLE I

The expression of a subset of PDGF-inducible genes is inhibited by the SFK-specific inhibitor SU6656

Quiescent NIH3T3 cells were treated for 1 h with 25 ng/ml PDGF or vehicle in the presence of 2 μM SU6656 or vehicle. Global patterns of gene expression were identified using Affymetrix Murine Genome U74Av2 GeneChip arrays. Gene expression data were normalized to an average intensity of 500 across each array, and the normalized CHP files were entered into xenobase, a relational database with associated analysis software. Gene expression ratios were $\log_2$-transformed prior to analysis so that relative increases and decreases in gene expression are represented on a linear scale. Gene expression data were analyzed using the following filters: expression values were present in all samples; values differed by more than 100 intensity units from reference; values were equal to or greater than 50 units, and values were increased at least 2-fold in response to PDGF. This filtering resulted in the inclusion of 127 probe IDs that were induced at least 2-fold by PDGF, and of these 36 were induced less than 1.5-fold in response to PDGF plus 2 μM SU6656. The list of these SU6656-responsive probe IDs is shown, as is the percentage of SU6656-mediated inhibition.

Unigene	Gene encodes	$\log_2$ gene expression ratio relative to quiescent fibroblasts		Percent inhibition
		PDGF	PDGF + SU6656	
Mm.4679	Glial cell line-derived neurotrophic factor	140.0	21.8	84.4
Mm.289824	Interleukin 1 receptor-like 1	32.7	5.2	84.3
M19681	MCP-1	5.1	2.0	61.4
Mm.328358	cDNA clone UI-M-BH1-alc-a-02-0-UI 5′	4.3	1.9	56.5
U20735	JunB	3.3	1.5	53.9
Mm.259672	Adult male aorta and vein cDNA, RIKEN full-length enriched library, clone: A530041M22	3.0	1.4	52.8
L00039	Myc	14.3	6.8	52.3
Mm.290207	E26 avian leukemia oncogene 2, 3′-domain	3.7	1.8	51.9
Mm.1408	Adrenomedullin	21.8	10.6	51.6
Mm.86541	CCR-4	16.1	7.8	51.2
D16497	Natriuretic peptide precursor type B	14.0	7.2	48.9
Mm.795	Colony-stimulating factor 1 (macrophage)	2.5	1.3	48.4
Mm.3468	Suppressor of cytokine signaling 3	3.0	1.6	47.8
U89411	Nuclear factor, interleukin 3, regulated	17.5	9.3	47.0
Mm.24402	Glutamine fructose-6-phosphate transaminase 2	23.7	12.7	46.6
Mm.18571	Tis 11b	5.1	2.8	45.0
U83148	Nuclear factor, interleukin 3, regulated	2.0	1.1	44.3
Mm.8042	Inhibin β-A	4.0	2.3	42.4
Mm.3117	Pleckstrin homology-like domain, family A, member 1	4.7	2.8	41.7
Mm.282184	Vascular endothelial growth factor A	5.4	3.1	41.6
Mm.25613	Immediate early response 3	3.3	2.0	40.6
U86783	Nuclear receptor subfamily 4, group A, member 2	46.5	27.9	40.1
Mm.280895	Uridine monophosphate kinase	2.3	1.4	39.7
Mm.26147	11 days embryo head cDNA, RIKEN full-length Enriched library, clone: 6230421P05 product: unknown EST, full insert sequence	2.6	1.6	37.5
K02236	Metallothionein 2	39.9	25.2	36.7
U20735	JunB	3.4	2.2	36.2
AV374868	Suppressor of cytokine signaling 3	2.1	1.3	36.1
M28845	Egr-1	2.5	1.6	35.8
Mm.292547	Prostaglandin-endoperoxide synthase 2	4.0	2.6	35.3
Mm.249333	RIKEN cDNA 1300002F13 gene	4.7	3.1	34.8
Mm.110220	DNA-damage inducible transcript 3	9.5	6.2	34.8
U86783	Nuclear receptor subfamily 4, group A, member 2	2.3	1.5	34.6
Mm.2706	Activating transcription factor 3	2.1	1.4	34.2
Mm.289824	Interleukin 1 receptor-like 1	11.6	7.7	34.0
X70058	MCP-3	2.5	1.6	33.7
V00835	Metallothionein 1	3.0	2.0	33.6

The $\log_2$-transformed gene expression ratios from experiment 1 were plotted against the $\log_2$-transformed gene expression ratios from experiment 2. The resulting correlation coefficient of 0.87 demonstrated a high level of experimental reproducibility between experiments (Fig. 1*A*). This set of probe IDs was further filtered to include only probe IDs that changed expression levels at least 2-fold in response to PDGF treatment. Again, the $\log_2$-transformed gene expression ratios from experiment 1 were plotted against the $\log_2$-transformed gene expression ratios from experiment 2. In this case, the correlation coefficient of 0.89 further demonstrated a low level of variability in gene expression data between experiments (Fig. 1*B*).

PDGF Drives Pathway-specific Gene Expression—To determine the contribution of various signaling pathways to PDGF-induced immediate early gene expression, we analyzed global patterns of PDGF-induced gene expression in the presence of various small molecule inhibitors. Because we were most interested in the contribution of SFKs in PDGF-induced gene expression, we used the drug SU6656 to block SFK activity (9). To isolate the contribution of SFKs specifically, PDGF-induced gene expression was also analyzed in the presence of the MEK1/2 inhibitors U0126 or PD98059, or in the presence of the PI3K inhibitor LY294002. The concentrations of inhibitors were selected based on the minimum concentrations of each drug required to completely block PDGF-induced bromodeoxyuridine incorporation in NIH3T3 cells (data not shown).

To demonstrate that inhibitor treatment alone has little effect on overall gene expression levels, quiescent NIH3T3 cells were treated for 1 h with 25 ng/ml PDGF or vehicle in the presence of 2 μM SU6656, 10 μM U0126, 7.5 μM LY294002, or vehicle. Total RNA was hybridized to Affymetrix Mouse Expression (MOE) 430A GeneChip arrays as described under "Experimental Procedures." We analyzed gene expression data by using the following filters: gene expression values were present in all samples; sample intensity values were greater than 50 units and differed by more than 100 intensity units from reference values, and sample values varied at least 3-fold with respect to quiescent NIH3T3 reference. This filtering resulted in the inclusion of 29 different probe IDs. Some genes were represented by multiple probe IDs (*e.g.* Tis 11b, Krupple-like factor 4, etc.), which provides additional confirmation of their expression patterns. These 29 probe IDs were subjected to unsupervised hierarchical clustering so that changes in gene expression across samples could be readily observed. The clus-

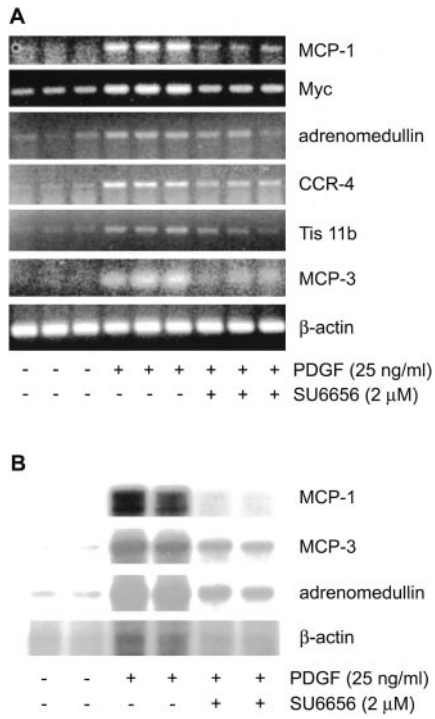

FIG. 3. **RT-PCR and RPA analysis of PDGF-inducible genes.** Quiescent NIH3T3 cells were treated for 1 h with 25 ng/ml PDGF or vehicle in the presence of 2 μM SU6656 or vehicle. *A*, by using equivalent amounts of cDNA for each reaction, gene-specific primer pairs were used to amplify small segments of genes by PCR. Reactions were performed in triplicate, and β-actin was used as a control for relative amounts of template cDNA. *B*, ribonuclease protection assays were performed using gene-specific probes. Reactions were performed in duplicate, and β-actin was used as a control for relative amounts of total RNA.

ter diagram of these data, which were not mean-centered, indicates relative high and low expression for the given probe ID as shown in Fig. 2 by *red* and *green boxes*, respectively. These data demonstrate that each inhibitor alone has little effect on basal levels of gene expression and that PDGF treatment induces the expression of a set of genes, which are differentially affected by inhibitors. Note that whereas LY294002 alone appears to significantly alter expression of a few probe IDs in clustering raw data, in fact when clustering mean-centered data, these differences are less significant.

SFK-dependent Genes—To identify a set of PDGF-induced immediate early genes that required SFK activity for expression, quiescent NIH3T3 cells were treated for 1 h with 25 ng/ml PDGF or vehicle in the presence of 2 μM SU6656 or vehicle. Global patterns of gene expression were analyzed using Affymetrix MG U74Av2 GeneChip arrays using the following filters: values were present in all samples; sample intensity values were equal to or greater than 50 units and differed by more than 100 units from reference, and sample values were increased at least 2-fold in response to PDGF. This filtering resulted in the inclusion of 127 probe IDs that were induced at least 2-fold by PDGF, and of these 36 were induced less than 1.5-fold in response to PDGF plus 2 μM SU6656 (Table I).

We performed semi-quantitative RT-PCR as well as RPA analysis to validate these gene expression data. By using equivalent amounts of cDNA for each reaction, gene-specific primer pairs were used to amplify small segments of the genes of interest by PCR as described under "Experimental Procedures." Six genes were selected for RT-PCR analysis because the array analysis suggested their expression was induced by PDGF and inhibited by SU6656 (Table I). Reactions were performed in triplicate, and β-actin was used as a control for relative amounts of template. These data demonstrate that

TABLE II

The expression of discrete sets of PDGF-responsive genes is specifically inhibited by the SFK inhibitor SU6656, by the MEK inhibitor U0126, and by the PI3K inhibitor LY294002

Quiescent NIH3T3 cells were treated for 1 h with 25 ng/ml PDGF or vehicle in the presence of 2 μM SU6656, 10 μM U0126, 7.5 μM LY294002, or vehicle. Global patterns of gene expression were identified using Affymetrix MOE 430A GeneChip arrays (for details see Table I). Gene expression data were analyzed using the following filters: values were present in all samples; values differed by more than 100 intensity units from reference; values were increased at least 2-fold in response to PDGF, and values were decreased at least 50% in response to only one of three inhibitors. This filtering resulted in the inclusion of 174 probe IDs that were induced at least 2-fold by PDGF, and of these 6 were specifically inhibited at least 50% by 2 μM SU6656, 11 were specifically inhibited at least 50% by 10 μM U0126, and 2 were specifically inhibited at least 50% by 7.5 μM LY294002. The list of these probe IDs is shown.

Unigene	Gene encodes	Log_2 gene expression ratio relative to quiescent fibroblasts			
		PDGF	PDGF + SU6656	PDGF + U0126	PDGF + LY294002
SFK-dependent					
Mm.290320	MCP-1	28.4	8.9	21.1	40.0
Mm.246513	Fos	12.3	4.4	17.0	13.1
Mm.86541	CCR-4	25.8	10.2	18.3	22.0
Mm.1408	Adrenomedullin	2.7	1.2	3.2	3.8
Mm.795	Colony-stimulating factor 1 (macrophage)	3.4	1.6	2.2	3.1
Mm.259672	Adult male aorta and vein cDNA, RIKEN full-length enriched library, clone: A530041M22	3.5	1.7	3.3	5.5
MEK-dependent					
Mm.282092	Hsp40	9.2	6.8	2.0	8.8
Mm.282092	Hsp40	6.1	4.3	1.6	6.1
Mm.248335	FosB	16.1	16.7	4.7	13.7
Mm.249333	RIKEN cDNA 1300002F13 gene	24.9	13.4	7.4	23.7
Mm.6215	Fra-1	18.0	14.1	5.6	15.8
Mm.249333	RIKEN cDNA 1300002F13 gene	36.5	20.9	14.4	38.9
Mm.4791	Epiregulin	13.5	11.0	5.4	16.6
Mm.289681	Diphtheria toxin receptor	12.4	7.3	5.1	15.7
Mm.6215	Fra-1	11.7	9.1	5.0	10.1
Mm.290421	Egr-2	13.3	9.8	5.7	11.3
Mm.28405	Serum/glucocorticoid-regulated kinase	8.1	4.9	3.8	7.7
PI3K-dependent					
Mm.273188	Coagulation factor III	3.2	2.6	3.6	1.5
AV260654	AV260654	2.3	2.3	2.6	1.1

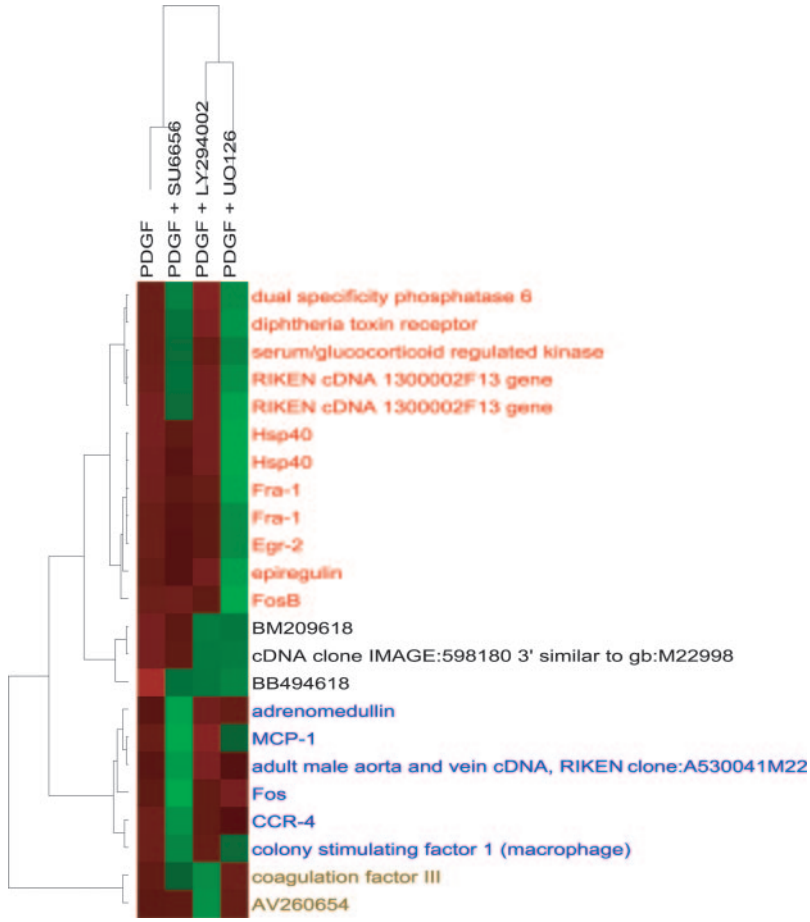

FIG. 4. **Hierarchical clustering of gene expression data of PDGF-inducible genes.** Quiescent NIH3T3 cells were treated for 1 h with 25 ng/ml PDGF or vehicle in the presence of 2 μM SU6656, 10 μM U0126, 7.5 μM LY294002, or vehicle. Global patterns of gene expression were identified by using Affymetrix Mouse Expression 430A GeneChip arrays, and gene expression ratios were $\log_2$-transformed prior to analysis so that relative increases and decreases in gene expression are represented on a linear scale. Expression data were filtered to include only those probe IDs whose expression was induced at least 2-fold in response to PDGF, with respect to quiescent NIH3T3 reference, and was reduced at least 2-fold in response to inhibitor. These data were subjected to mean-centered unsupervised hierarchical clustering so that relative changes in gene expression across samples could be readily observed. *Red* and *green boxes* indicate relative high and low expression, respectively, for the given probe ID. Probe IDs responsive to 2 μM SU6656 are labeled in *blue*; probe IDs responsive to 10 μM U0126 are labeled in *red*, and probe IDs responsive to 7.5 μM LY294002 are labeled in *brown*.

expression of *mcp-1*, *myc*, *adrenomedullin*, *ccr-4*, *tis 11b*, and *mcp-3* genes were enhanced in response to PDGF treatment and that in each case 2 μM SU6656 inhibited the PDGF-induced increase in gene expression (Fig. 3*A*). We then selected three of these six genes and analyzed expression levels further by using quantitative RPA. These data confirm that mRNA expression levels of MCP-1, MCP-3, and adrenomedullin were significantly increased in response to PDGF and were potently inhibited by SU6656 (Fig. 3*B*). The apparent small PDGF-induced increase in the expression of β-actin is likely because of the simultaneous use of four different riboprobes in this experiment, and we generally do not see very significant increases in β-actin expression in response to PDGF treatment (see Fig. 5*B*). These data confirm the gene expression data shown in Table I and validate the identity of a set of genes induced by PDGF through SFK activity.

We identified a set of PDGF-inducible genes that signal through SFKs. However, SFKs are known to also participate in signaling through other pathways, notably the Ras-MAPK pathways and the PI3K pathways (2). To determine which genes were specifically dependent on SFK activity for increased expression in response to PDGF, quiescent NIH3T3 cells were treated with 25 ng/ml PDGF or vehicle for 1 h in the presence of 2 μM SU6656, 10 μM U0126, 7.5 μM LY294002, or vehicle. For these analyses, gene expression was evaluated by using a newer version of the Affymetrix GeneChip arrays (MOE 430A) as described under "Experimental Procedures." Expression data were analyzed using the following filters: values were present in all samples; sample intensity values were greater than 50 units and differed by more than 100 intensity units from reference; sample values genes were increased at least 2-fold in response to PDGF treatment, and genes were inhibited at least 50% by one of the three inhibitors. This filtering resulted in the inclusion of 174 probe IDs that were induced at least 2-fold by PDGF, and of these 6 were only inhibited at least 50% by 2 μM SU6656, 11 were only inhibited at least 50% by 10 μM U0126, and 2 were only inhibited at least 50% by 7.5 μM LY294002 (Table II). All of the 23 probe IDs that passed the above filtering criteria were subjected to unsupervised hierarchical clustering so that changes in gene expression across samples could be readily observed. The cluster diagram of these mean-centered data indicates relative high and low expression for the given probe ID as shown in Fig. 4 by *red* and *green boxes*, respectively. These data demonstrate that each inhibitor alone has little effect on basal levels of gene expression and that PDGF treatment induces the expression of a set of genes, which are differentially affected by inhibitors.

We used semi-quantitative RT-PCR and RPA to validate these gene expression data as described above. RT-PCRs were performed in triplicate, and β-actin was used as a control for relative amounts of template cDNA. Expression levels of four putative SFK-specific genes (*mcp-1*, *fos*, *ccr-4*, and *adrenomedullin*) were greatly reduced by SU6656 but only slightly affected by U0126 or LY294002 (Fig. 5*A*). In contrast, expression levels of four putative MEK-specific genes (*hsp40*, *fra-1*, *epiregulin*, and *egr-2*) were greatly reduced by U0126 but only slightly by SU6656 or LY294002 (Fig. 5*A*). These results were further confirmed by using quantitative RPA analysis. Specifically, mRNA levels of MCP-1 and adrenomedullin were enhanced in response to PDGF treatment, but levels were reduced by treatment with 2 μM SU6656 (Fig. 5*B*). FosB and Fra-1 mRNA levels were also increased by PDGF treatment, but in this case expression was specifically inhibited by 10 μM U0126 (Fig. 5*B*).

Several of the PDGF-inducible genes that we had previously identified as being selectively responsive to SU6656 when us-

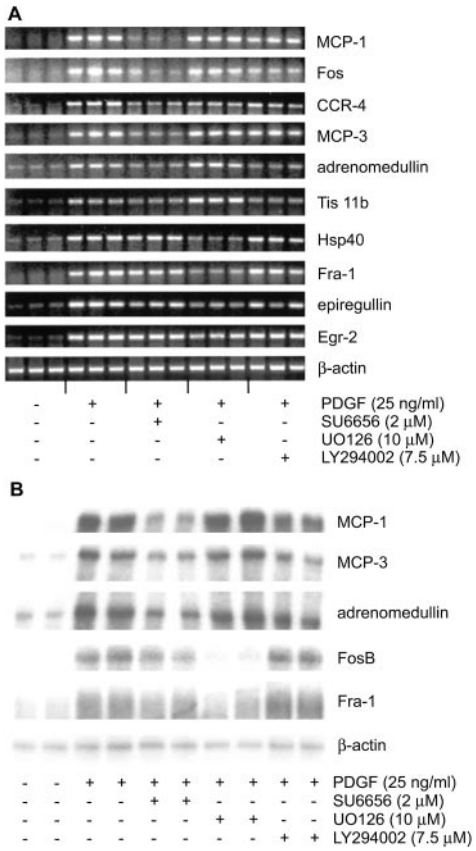

FIG. 5. **RT-PCR and RPA analysis of SFK-dependent and MEK-dependent genes.** Quiescent NIH3T3 cells were treated for 1 h with 25 ng/ml PDGF or vehicle in the presence of 2 μM SU6656, 10 μM U0126, 7.5 μM LY294002, or vehicle. *A*, by using equivalent amounts of cDNA for each reaction, gene-specific primer pairs were used to amplify small segments of genes by PCR. Reactions were performed in triplicate, and β-actin was used as a control for relative amounts of template cDNA. *B*, ribonuclease protection assays were performed using gene-specific probes. Reactions were performed in duplicate, and β-actin was used as a control for relative amounts of total RNA. The data presented are derived from two separate assays, each of which had internal positive and negative controls.

ing the MG U74Av2 chip (Table I and Fig. 3) failed to pass the stringent filtering criteria used when analyzing expression data using the MOE 430A chip (data not shown). We therefore directly tested the effects of the other kinase inhibitors on two of the genes that we had previously identified, *mcp-3* and *tis 11b*, using RT-PCR, as well as RPA in the case of MCP-3. Expression levels of both genes were induced in response to PDGF, inhibited significantly by SU6656, and only slightly inhibited by U0126 or LY294002 (Fig. 5, *A* and *B*). In sum, these results suggest that PDGF regulates immediate early gene expression by signaling through a discrete SFK pathway, which is at least somewhat distinct from the Ras-MAPK and PI3K pathways.

MEK-dependent Genes—Our data demonstrate that PDGF-induced expression of some genes was dependent on MEK activity. To confirm that the small molecule inhibitors in our model system are regulating gene expression through specific inhibition of the intended signaling proteins, we compared the effects of two different MEK1/2 inhibitors on PDGF-stimulated gene expression. Quiescent NIH3T3 cells were treated with 25 ng/ml PDGF or vehicle for 1 h in the presence of 10 μM U0126, 50 μM PD98059, or vehicle. Global patterns of gene expression were analyzed by using Affymetrix MG U74Av2 GeneChip arrays. Expression data were analyzed by using the following filters: values were present in all samples; sample intensity values were greater than 50 units and differed by more than 100 intensity units from reference; and sample values were increased at least 2-fold in response to PDGF, and increased no more than 1.5-fold by one or by both of the inhibitors. This filtering resulted in the inclusion of 189 probe IDs that were induced at least 2-fold by PDGF, and of these 19 were induced no more than 1.5-fold in the presence of 10 μM U0126 or 50 μM PD98059, 11 were induced no more than 1.5-fold in the presence of 10 μM U0126 alone, and 14 were induced no more than 1.5-fold in the presence of 50 μM PD98059 alone (Table III). Generally, the same genes were inhibited by both MEK1/2 inhibitors, even though in some cases the level of inhibition failed to rise above the filtering criteria (data not shown). However, there were notable exceptions. For example, the expression data suggested that Fra-1 was PDGF-inducible and responsive to both U0126 and PD98059 but that Btg-2 was PDGF-inducible and responsive to U0126 but not PD98059 (Table III).

RT-PCR was used to validate these gene expression data. RT-PCRs were performed in duplicate, and β-actin was used as a control for relative amounts of template cDNA. PDGF-induced expression levels of Fra-1 were potently inhibited by 10 μM U0126 as well as by 50 μM PD98059, but the PDGF-induced expression of Btg-2 was inhibited only by 10 μM U0126 (Fig. 6*A*). To confirm that both inhibitors were blocking MEK1/2 activity in our model system at the concentrations used, quiescent NIH3T3 cells were treated with increasing durations of 25 ng/ml PDGF as indicated in the presence of 10 μM U0126, 50 μM PD98059, or vehicle. MEK1/2 activity was assayed by immunoblotting for activated (tyrosine-phosphorylated) ERK1/2. PDGF rapidly induced ERK2 phosphorylation (within 5 min), and this phosphorylation was completely blocked by either 10 μM U0126 or 50 μM PD98059 (Fig. 6*B*). In addition, 2 μM SU6656 had no effect on PDGF-stimulated ERK1/2 phosphorylation (Fig. 6*B*). These results suggest that most PDGF-induced and putative MEK1/2-specific genes are sensitive to two different MEK1/2 inhibitors but with some notable exceptions. This might reflect the fact that the inhibitors we used are not totally selective for MEK1/2 and also inhibit other kinases. For example, 10 μM U0126 also potently inhibits MEK5 (and phosphorylation of its substrate, ERK5) in EGF- and hepatocyte growth factor-treated renal epithelial cells and HeLa cells (14, 15). In contrast, PD98059 only effectively inhibits MEK5 activation in EGF-treated cells at concentrations higher than those reported here (14, 15). Similarly, PD98059 may also bind and inhibit specific target molecules. For example, PD98059 has been reported to inhibit cyclooxygenases I and II, even though U0126 failed to inhibit these enzymes even at concentrations that completely block MAPK activation (16, 17).

PDGF Enhances the mRNA Stability, but Not the Transcription, of SFK-specific Genes—myc, which was identified as a PDGF-inducible and SFK-specific gene in the current screen (Table I), has been an ongoing gene of interest in our laboratory (4, 9, 10). It has been shown previously (18) that serum growth factors regulate expression of the *myc* gene primarily at the level of mRNA stability, rather than at the level of gene transcription. To test whether PDGF also promotes *myc* mRNA increases through stabilization, and whether other PDGF-inducible and SFK-specific genes are similarly regulated, we used nuclear run-off assays to measure the rates of transcription for a subset of PDGF-inducible and SFK-specific genes. The rate of transcription of the *myc* gene was detectable in quiescent NIH3T3 cells, and it did not change in response to PDGF over a period of 0–60 min (Fig. 7*A*). As a control, we collected the material comprising the cytosolic fraction of the cell lysate from these run-off assays (containing total RNA) and used RPA to

TABLE III

The expression of a subset of PDGF-inducible genes is responsive to the MEK inhibitors U0126 and PD98059

Quiescent NIH3T3 cells were treated for 1 h with 25 ng/ml PDGF or vehicle in the presence of 10 μM U0126, 50 μM PD98059, or vehicle. Global patterns of gene expression were identified using Affymetrix MOE 430A GeneChip arrays (for details see Table I). Gene expression data were analyzed using the following filters: values were greater than 50 units; values differed by more than 50 intensity units from reference; values were increased at least 2-fold in response to PDGF, and values were increased no more than 1.5-fold by PDGF in the presence of inhibitor. This filtering resulted in the inclusion of 150 probe IDs that were induced at least 2-fold by PDGF, and of these 11 were induced less than 1.5-fold by PDGF in the presence of 10 μM U0126, 14 were induced less than 1.5-fold by PDGF in the presence of 50 μM PD98059, and 19 were induced less than 1.5-fold by PDGF in the presence of either 10 μM U0126 or 50 μM PD98059. The list of these probe IDs is shown.

Unigene	Gene encodes	Log_2 gene expression ratio relative to quiescent fibroblasts		
		PDGF	PDGF + U0126	PDGF + PD98059
U0126- and PD98059-responsive				
Mm.1359	Urokinase plasminogen activator receptor	3.6	2.4	1.9
Mm.248335	FosB	8.2	2.0	4.4
Mm.24096	Thrombomodulin	3.4	2.2	1.7
Mm.279106	Cofactor required for Sp1 transcriptional activation, subunit 8	2.0	1.3	1.2
Mm.3117	Pleckstrin homology-like domain, family A, member 1	20.1	9.2	6.0
AV381829	AV381829	3.6	1.7	2.3
Mm.289681	Diphtheria toxin receptor	3.9	1.8	1.4
Mm.4863	Ubiquitin-conjugating enzyme E2 variant 1	2.4	1.4	1.6
Mm.1791	Dual specificity phosphatase 6	31.9	9.2	9.8
Mm.249333	RIKEN cDNA 1300002F13 gene	35.1	7.9	20.0
Mm.249333	RIKEN cDNA 1300002F13 gene	24.2	7.5	11.1
Mm.246398	TCDD-inducible poly(ADP-ribose) polymerase	13.4	6.3	6.9
Mm.330818	Semaphorin 4B precursor	3.3	1.3	0.6
Mm.295252	Peptidylprolyl isomerase D (cyclophilin D)	2.3	1.2	1.3
AW046181	AW046181	4.1	2.1	2.3
Mm.289824	Interleukin 1 receptor-like 1	6.4	1.9	2.2
Mm.289824	Interleukin 1 receptor-like 1	4.6	1.9	1.3
Mm.89888	Glutamate-cysteine ligase, catalytic subunit	2.5	1.3	1.3
AF017128	Fra-1	10.7	5.0	5.1
U0126-responsive				
U70475	Nuclear factor, erythroid derived 2, like 2	2.4	1.4	1.8
Mm.101034	TG-interacting factor	5.0	2.9	4.0
Mm.1167	JunB oncogene	20.3	12.1	15.0
Mm.300399	SOCS-5 mRNA, complete cds	2.3	1.4	2.7
Mm.227	Integrin αV	3.3	2.1	3.8
Mm.86541	CCR-4	13.4	8.5	12.7
Mm.239605	Btg-2	9.6	6.2	8.9
Mm.2093	Snail homolog 1 (*Drosophila*)	2.2	1.4	1.6
Mm.227506	DNA segment, Chr 7, ERATO Doi 458, expressed	10.6	6.8	11.9
Mm.290421	Egr-2	20.8	13.6	14.9
Mm.4499	Calcium channel, voltage-dependent, L-type, α1C subunit	2.4	1.6	1.9
PD98059-responsive				
Mm.25613	Immediate early response 3	16.6	16.4	7.1
Mm.272602	CCAAT/enhancer-binding protein (C/EBP), δ	5.0	3.7	2.3
Mm.292547	Prostaglandin-endoperoxide synthase 2	16.7	16.5	8.3
Mm.6522	Chemokine orphan receptor 1	2.2	1.6	1.1
Mm.239041	Dual specificity phosphatase 1	2.3	2.5	1.2
V00727	Fos	18.6	17.0	10.0
AF004100	Solute carrier family 30 (zinc transporter), member 4	2.1	1.5	1.2
Mm.8042	Inhibin β-A	4.1	3.3	2.4
L00039	Myc	7.6	5.3	4.4
Mm.4660	Chemokine (CXC motif) ligand 5	2.1	1.7	1.2
Mm.164948	Ecotropic viral integration site 2B	2.2	2.0	1.3
Mm.1068	B-cell leukemia/lymphoma 3	2.1	1.6	1.3
AV374868	Similar to suppressor of cytokine signaling-3	5.6	4.7	3.5
D16497	Natriuretic peptide precursor type B	3.7	3.0	2.3

confirm that *myc* mRNA was indeed increased in response to PDGF treatment (Fig. 7*B*). These data confirm the stabilization of *myc* mRNA in response to growth factors and further suggest SFKs may be involved in regulating mRNA stability.

Providing further evidence for this mechanism, transcription of both *mcp-1* and *mcp-3* genes was also high in quiescent NIH3T3 cells and was unaffected by PDGF treatment (Fig. 7*A*), even though we demonstrated that these genes were induced in

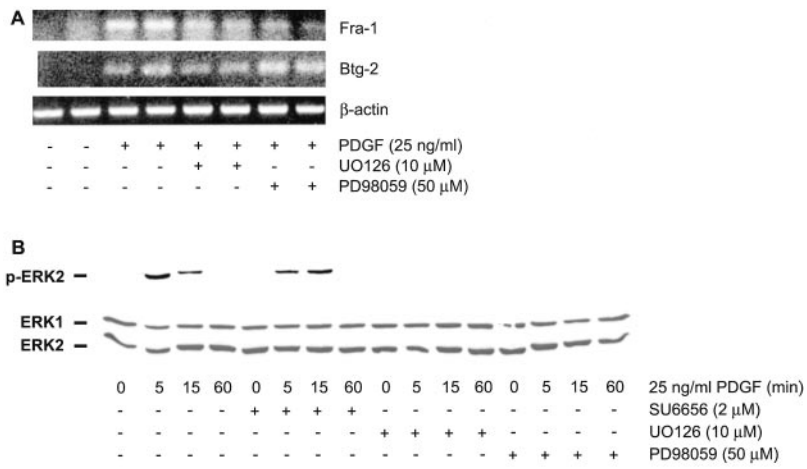

FIG. 6. **RT-PCR and Western blot analysis validates genes likely to be PDGF-inducible and responsive to MEK inhibitors U0126 and PD98059.** *A*, quiescent NIH3T3 cells were treated for 1 h with 25 ng/ml PDGF or vehicle in the presence of 10 μM U0126, 50 μM PD98059, or vehicle. By using equivalent amounts of cDNA for each reaction, gene-specific primer pairs were used to amplify small segments of genes by PCR. Reactions were performed in duplicate, and β-actin was used as a control for relative amounts of template cDNA. *B*, quiescent NIH3T3 cells were stimulated for 0–60 min with 25 ng/ml PDGF in the presence or absence of 2 μM SU6656, 10 μM U0126, 50 μM PD98059, or vehicle as indicated. Levels of phospho-ERK1/2 and total ERK1/2 protein were measured using SDS-PAGE and immunoblotting.

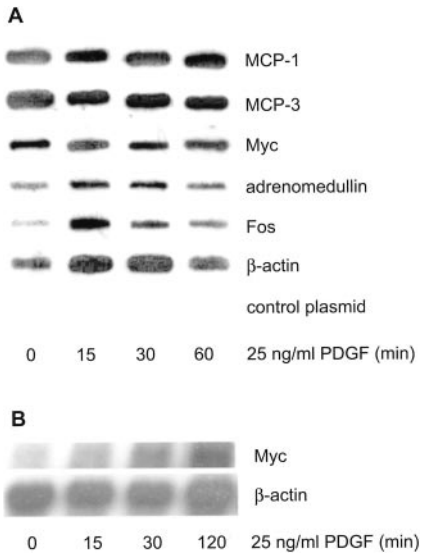

FIG. 7. **RPA and nuclear run-off analyses of SFK-specific genes.** Quiescent NIH3T3 cells were treated with 25 ng/ml PDGF for increasing amounts of time as indicated. *A,* nuclei were isolated and levels of *mcp-1*, *mcp-3*, *myc*, *adrenomedullin*, *fos*, and *β-actin* gene transcription were analyzed using nuclear run-off assays. Data are taken from three separate run-off assays, each of which had internal positive and negative controls. *B,* cytoplasmic fractions of cell lysates were obtained, total RNA was isolated for each time point, and levels of *myc* and *β-actin* mRNAs were determined by RPA.

response to PDGF specifically through SFKs (Table II and Figs. 3 and 5). The transcription of *adrenomedullin*, another PDGF-inducible and SFK-specific gene, was also only slightly responsive to PDGF (Fig. 7*A*). Finally, as a control for the run-off assay, we determined rates of *fos* transcription in response to PDGF. Previous data have shown that it is primarily *fos* transcription that is induced in response to growth factor stimulation (18), and we confirmed that *fos* transcription was highly induced by PDGF treatment in our model system (Fig. 7*A*). In sum, these data suggest that in response to growth factor the role of SFKs is to signal stabilization of target mRNAs.

DISCUSSION

Our laboratory has recently focused on one particular output of SFK activity, the growth factor-stimulated production of Myc, a transcription factor required for efficient cell cycle transit. Previous work demonstrated that the block to PDGF-stimulated DNA synthesis caused by dominant negative SFKs could be overcome by expression of Myc (10). Another transcription factor, Fos, was unable to rescue this block. Furthermore, Myc could not overcome the block caused by dominant negative Ras. Together, these data suggested that SFKs initiate a signal transduction pathway, distinct from the classical Ras-MAPK pathway, which culminates in Myc production. The subsequent characterization and use of SU6656, an SFK inhibitor, confirmed that *myc* mRNA was in large part under SFK control (9).

In fibroblasts, early reports suggested that PDGF increased levels of *myc* mRNA by increasing the rate of *myc* transcription (19, 20). However, others have shown that the basal transcription rate of *myc* in quiescent fibroblasts is high, and it is unchanged by stimulation with serum or thrombin (21–24). This suggests that it is primarily the stability of *myc* mRNA that is affected by mitogens. Our data confirm that it is this mRNA stability mechanism that operates in NIH3T3 cells in response to PDGF stimulation. Our data also identify other short lived SFK-specific RNAs (MCP-1, MCP-3, and adrenomedullin) that are regulated primarily by enhanced mRNA stability. In the case of MCP-1, PDGF has been reported to increase *mcp-1* mRNA stability/levels in vascular smooth muscle cells (25), although increases in *mcp-1* transcription in response to PDGF have also been detected in these cells (26). There are also data to suggest that MCP-3 and adrenomedullin expression are also regulated by mRNA stabilization, but what roles PDGF or SFKs might play in those processes is unclear (27, 28).

The control of the stability of short lived mRNAs is under intense scrutiny, but how mitogenic signals impact this control is not yet fully understood. Previous work has demonstrated how the half-life of *myc* mRNA is regulated. Two regions, one in the 3′-untranslated region (UTR) and one in the coding region (CR), are involved (29, 30). The CR instability determinant (CRD) in the *myc* CR targets *myc* mRNA for endonuclease attack during translational pausing (31). A CRD-binding protein has been identified, which shields this region. CRD-binding protein is a member of the family of KH domain-containing RNA-binding proteins (32, 33). It is highly expressed in fetal tissues and in some cancer cell lines, and its expression may in part explain high levels of Myc protein in these cases (34). However, CRD-binding protein has not been detected in normal adult cells, including fibroblasts. The 3′-UTR of the *myc* gene contains AU-rich elements (AUREs) that are frequently found in unstable mRNAs (35). Several AURE-binding proteins have been described. Some (such as HuR) stabilize and some (such as AUF1 and tristetraprolin) destabilize transcripts (30). However, little is known regarding the influence of signaling pathways on *myc* AURE-binding proteins. Most interestingly, one of the SFK-specific PDGF-inducible genes we identified, Tis 11b, is related to tristetraprolin and has recently been shown to destabilize vascular endothelial growth factor mRNA in re-

sponse to adrenocorticotropic hormone (36). Thus, it is possible that Tis 11b might also play a role in SFK-mediated mRNA stability of *myc* or of other SFK-dependent genes. Furthermore, the instability determinant need not be restricted to the 3′-UTR. *mcp-1* mRNA, for example, contains a region within its 5′-UTR that appears to destabilize the mRNA in response to PDGF plus dexamethasone (37).

A recent report suggested that PDGF signals immediate early gene expression with little or no specificity with regard to signaling pathways. In this study, NIH3T3 cells were transfected with wild-type PDGF-R or with a number of receptor mutants that contained amino acid substitutions at sites that mediate interaction with various signaling effectors, including the Ras/MAPK and PI3K pathways. These investigators found that, in response to PDGF-R activation, wild-type and mutant receptors promoted the expression of an identical set of 64 immediate early genes in fibroblasts (11). However, our data demonstrate that PDGF stimulation of SFK and MEK pathways each caused the increased expression of a specific set of immediate early genes. In particular, we isolated a set of genes that were induced by PDGF through SFK activity but not MEK1/2 or PI3K. Furthermore, a recent report (38) described the PDGF-stimulated increase in expression of specific sets of genes in fibroblasts, including genes required for fatty acid and cholesterol biosynthesis, in a PI3K-dependent manner. Finally, a recent report (39) identified specific sets of genes that were induced in response to PDGF through either MEK or PI3K activity. What is the reason for the apparent discrepancy in these observations? The differences most likely arise from the differing methodologies employed. Fambrough *et al.* (11) mutated known PDGF-R effector-binding sites and then measured the effect that each mutant had on signaling gene expression in response to receptor activation. Although this approach can unambiguously determine whether stable association of signaling intermediates with the PDGF-R is required, it does not preclude the possibility that these proteins participate in PDGF signaling without association. We used pharmacological inhibitors of SFKs and other kinases, thus ensuring that all enzyme activity was blocked. It is also possible that receptor number and/or the concentration of PDGF used in these studies has a significant impact on the gene expression profiles detected. In our studies, we used 25 ng/ml PDGF (a submaximal but physiological dose) and unengineered cells, whereas Fambrough *et al.* (11) used cells engineered to express receptor mutants and saturating levels of growth factor.

Our data are in agreement with several other reports identifying serum- and PDGF-inducible genes (38–41). In particular, many of the PDGF-inducible genes we identified (*e.g. junB*, *tis 11b*, *fra-1*, *mcp-1*, *myc*, etc.) were also described in a recent report (38) analyzing gene expression in fibroblasts induced by 1–24 h of PDGF treatment. Many of the PI3K-dependent genes these investigators identified were induced only after 24 h of growth factor stimulation. Because we measured gene expression after just 1 h of PDGF treatment, this might explain how we failed to detect PDGF-inducible, PI3K-dependent genes.

A recent report (42) used Affymetrix GeneChip analysis to identify a set of genes that are induced in Src-transformed cells. Many of the Src-transformed genes identified were also up-regulated in colon tumors. Generally, only a few of the genes we identified are represented in this "Src transformation fingerprint" (data not shown). We have also analyzed gene expression patterns in fibroblasts transformed with an activated form of Src (Src^{Y527F}), and we compared this pattern of expression with PDGF-inducible genes generally and SFK-dependent genes specifically. We also detected very little overlap in the patterns of gene expression. Only a few of the PDGF-inducible and SFK-dependent genes we identified in the current study were overexpressed in Src-transformed fibroblasts, and the pattern of gene expression in Src-transformed cells was very different from PDGF-induced gene expression.[2] These data suggest that transformation drives a different set of genes than growth factor stimulation. This is possibly because many genes may be induced secondarily in response to Src transformation and not primarily because of SFK activity *per se*.

In summary, microarray analysis has revealed a distinct set of mRNAs whose increased expression in response to PDGF is dependent upon SFKs. Most interestingly, many of these genes are regulated at the level of mRNA stabilization. One of these genes is *myc*, whose product is a transcription factor required for mitogenesis. We have preliminary evidence[3] that PDGF stimulation of quiescent fibroblasts causes an SFK-dependent change in the composition of proteins binding to the AURE in the 3′-UTR of the *myc* gene. It will be important in the future to determine how SFKs regulate AURE-binding proteins.

Acknowledgments—We thank Rebecca Gordon for excellent assistance in this project. We thank James Darnell and members of the laboratory for advice on nuclear run-off assays. The Affymetrix GeneChips were processed at the Affymetrix Core of the Genomics Technology Support Facility at Michigan State University.

REFERENCES

1. Abram, C. L., and Courtneidge, S. A. (2000) *Exp. Cell Res.* **254,** 1–13
2. Thomas, S. M., and Brugge, J. S. (1997) *Annu. Rev. Cell Dev. Biol.* **13,** 513–609
3. Brown, M. T., and Cooper, J. A. (1996) *Biochim. Biophys. Acta* **1287,** 121–149
4. Bromann, P. A., Korkaya, H., and Courtneidge, S. A. (2004) *Oncogene* **23,** 7957–7968
5. Ralston, R., and Bishop, J. M. (1985) *Proc. Natl. Acad. Sci. U. S. A.* **82,** 7845–7849
6. Kypta, R. M., Goldberg, Y., Ulug, E. T., and Courtneidge, S. A. (1990) *Cell* **62,** 481–492
7. Mori, S., Ronnstrand, L., Yokote, K., Engstrom, A., Courtneidge, S. A., Claesson-Welsh, L., and Heldin, C. H. (1993) *EMBO J.* **12,** 2257–2264
8. Twamley-Stein, G. M., Pepperkok, R., Ansorge, W., and Courtneidge, S. A. (1993) *Proc. Natl. Acad. Sci. U. S. A.* **90,** 7696–7700
9. Blake, R. A., Broome, M. A., Liu, X., Wu, J., Gishizky, M., Sun, L., and Courtneidge, S. A. (2000) *Mol. Cell. Biol.* **20,** 9018–9027
10. Barone, M. V., and Courtneidge, S. A. (1995) *Nature* **378,** 509–512
11. Fambrough, D., McClure, K., Kazlauskas, A., and Lander, E. S. (1999) *Cell* **97,** 727–741
12. Miller, J., Bromberg-White, J. L., DuBois, K., Eugster, E., Srikanth, S., Haddad, R., DeLeeuw, C., and Webb, C. P. (2003) *Appl. Genomics Proteomics* **2,** 253–265
13. Eisen, M. B., Spellman, P. T., Brown, P. O., and Botstein, D. (1998) *Proc. Natl. Acad. Sci. U. S. A.* **95,** 14863–14868
14. Mody, N., Leitch, J., Armstrong, C., Dixon, J., and Cohen, P. (2001) *FEBS Lett.* **502,** 21–24
15. Karihaloo, A., O'Rourke, D. A., Nickel, C., Spokes, K., and Cantley, L. G. (2001) *J. Biol. Chem.* **276,** 9166–9173
16. Borsch-Haubold, A. G., Pasquet, S., and Watson, S. P. (1998) *J. Biol. Chem.* **273,** 28766–28772
17. Davies, S. P., Reddy, H., Caivano, M., and Cohen, P. (2000) *Biochem. J.* **351,** 95–105
18. Greenberg, M. E., and Ziff, E. B. (1984) *Nature* **311,** 433–438
19. Kelly, K., Cochran, B. H., Stiles, C. D., and Leder, P. (1983) *Cell* **35,** 603–610
20. Sacca, R., and Cochran, B. H. (1990) *Oncogene* **5,** 1499–1505
21. Nepveu, A., Levine, R. A., Campisi, J., Greenberg, M. E., Ziff, E. B., and Marcu, K. B. (1987) *Oncogene* **1,** 243–250
22. Dean, M., Levine, R. A., Ran, W., Kindy, M. S., Sonenshein, G. E., and Campisi, J. (1986) *J. Biol. Chem.* **261,** 9161–9166
23. Kindy, M. S., and Sonenshein, G. E. (1986) *J. Biol. Chem.* **261,** 12865–12868
24. Blanchard, J. M., Piechaczyk, M., Dani, C., Chambard, J. C., Franchi, A., Pouyssegur, J., and Jeanteur, P. (1985) *Nature* **317,** 443–445
25. Taubman, M. B., Rollins, B. J., Poon, M., Marmur, J., Green, R. S., Berk, B. C., and Nadal-Ginard, B. (1992) *Circ. Res.* **70,** 314–325
26. Bogdanov, V. Y., Poon, M., and Taubman, M. B. (1998) *J. Biol. Chem.* **273,** 24932–24938
27. Kakoki, M., Tsai, Y. S., Kim, H. S., Hatada, S., Ciavatta, D. J., Takahashi, N., Arnold, L. W., Maeda, N., and Smithies, O. (2004) *Dev. Cell* **6,** 597–606
28. Ren, L., and Syapin, P. J. (2002) *J. Pharmacol. Exp. Ther.* **303,** 265–272
29. Ross, J. (1995) *Microbiol. Rev.* **59,** 423–450
30. Guhaniyogi, J., and Brewer, G. (2001) *Gene (Amst.)* **265,** 11–23
31. Lemm, I., and Ross, J. (2002) *Mol. Cell. Biol.* **22,** 3959–3969
32. Doyle, G. A., Betz, N. A., Leeds, P. F., Fleisig, A. J., Prokipcak, R. D., and Ross, J. (1998) *Nucleic Acids Res.* **26,** 5036–5044
33. Ross, J., Lemm, I., and Berberet, B. (2001) *Oncogene* **20,** 6544–6550
34. Leeds, P., Kren, B. T., Boylan, J. M., Betz, N. A., Steer, C. J., Gruppuso, P. A.,

[2] P. A. Bromann and S. A. Courtneidge, unpublished observations.
[3] H. Korkaya and S. A. Courtneidge, unpublished observations.

and Ross, J. (1997) *Oncogene* **14,** 1279–1286
35. Xu, N., Chen, C. Y., and Shyu, A. B. (1997) *Mol. Cell. Biol.* **17,** 4611–4621
36. Ciais, D., Cherradi, N., Bailly, S., Grenier, E., Berra, E., Pouyssegur, J., Lamarre, J., and Feige, J. J. (2004) *Oncogene* **23,** 8673–8680
37. Poon, M., Liu, B., and Taubman, M. B. (1999) *Mol. Cell. Biol.* **19,** 6471–6478
38. Demoulin, J. B., Ericsson, J., Kallin, A., Rorsman, C., Ronnstrand, L., and Heldin, C. H. (2004) *J. Biol. Chem.* **279,** 35392–35402
39. Tullai, J. W., Schaffer, M. E., Mullenbrock, S., Kasif, S., and Cooper, G. M. (2004) *J. Biol. Chem.* **279,** 20167–20177
40. Iyer, V. R., Eisen, M. B., Ross, D. T., Schuler, G., Moore, T., Lee, J. C., Trent, J. M., Staudt, L. M., Hudson, J., Jr., Boguski, M. S., Lashkari, D., Shalon, D., Botstein, D., and Brown, P. O. (1999) *Science* **283,** 83–87
41. Chen, W. V., Delrow, J., Corrin, P. D., Frazier, J. P., and Soriano, P. (2004) *Nat. Genet.* **36,** 304–312
42. Malek, R. L., Irby, R. B., Guo, Q. M., Lee, K., Wong, S., He, M., Tsai, J., Frank, B., Liu, E. T., Quackenbush, J., Jove, R., Yeatman, T. J., and Lee, N. H. (2002) *Oncogene* **21,** 7256–7265